# FEM-based Reachable Workspace Estimation of Soft Robots using an Interval Analysis approach

Walid Amehri, Gang Zheng, Alexandre Kruszewski

▶ **To cite this version:**

Walid Amehri, Gang Zheng, Alexandre Kruszewski. FEM-based Reachable Workspace Estimation of Soft Robots using an Interval Analysis approach. Soft Robotics, In press. hal-03913432

**HAL Id: hal-03913432**
**https://inria.hal.science/hal-03913432**

Submitted on 27 Dec 2022

**HAL** is a multi-disciplinary open access archive for the deposit and dissemination of scientific research documents, whether they are published or not. The documents may come from teaching and research institutions in France or abroad, or from public or private research centers.

L'archive ouverte pluridisciplinaire **HAL**, est destinée au dépôt et à la diffusion de documents scientifiques de niveau recherche, publiés ou non, émanant des établissements d'enseignement et de recherche français ou étrangers, des laboratoires publics ou privés.

# FEM-based Reachable Workspace Estimation of Soft Robots using an Interval Analysis approach

Walid Amehri[1] and Alexandre Kruszewski[1]

[1] University of Lille, Inria, CNRS, Centrale Lille, UMR 9189 CRIStAL, F-59000 Lille, France

**Abstract**

Considering a soft robot with installed bounded actuators, this paper studies the reachable workspace estimation problem for a pre-chosen point of interest. To this aim, the method of finite-element has been used to obtain the static model of the studied robot and two methods are proposed (forward one which is based on Newton iterative method and forward-backward one which is based on interval analysis techniques) to study this estimation problem. Various simulations with different configuration scenarios are provided to show the effectiveness of the forward-backward approach which can largely reduce the exploration time, compared to the forward method.

***Keywords:*** Soft robotics; Reachable workspace; Finite-element method; Interval analysis

## 1 Introduction

Rigid robots utilize stiff materials to produce enough stiffness and are commonly used in the industry to increase productivity, which however suffer from safety problems when collaborating with human beings [1]. Therefore, researchers in the field of robotics have sought a new design of robots that can provide more functionality, flexibility, and safety in order to cope with new robotic applications [2, 3]. Being inspired from natural elements [4], soft robots represents the perfect instrument to operate in uncertain and dynamic environments [5] owing to their low stiffness and natural compliance. At the same time, as pointed out by [6], the classical procedure of designing a soft robot needs to be guided and optimized via the evaluation of their reachable workspace, while such an important subject has been rarely examined in this community.

In the field of rigid robotics, different approaches were explored to treat the workspace estimation problem for different types of rigid robots. An optimization method was presented in [7] to determine the boundaries of the workspace of rigid-link manipulators. A continuation method based on bifurcation theory has been stated in [8] to estimate the workspace boundaries of different rigid-link manipulators. In [9], a method based upon analytical analysis of Jacobian was developed to determine mechanism's singular behavior of the investigated rigid manipulator.

Also, the wrench-feasible workspace of parallel rigid robots driven by cables has been analyzed in [10] by applying an interval analysis bisection method. Such a method has been then extended to analyze the workspace of cable-suspended parallel rigid robots in [11,12]. Although the interval analysis based approaches have been successfully implemented in determining the workspace of several types of rigid robots, however they cannot be directly extended to analyze soft robots because of the complexity of the modeling of soft robots. In fact, the inputs/outputs relation (i.e., the actuation vector/the end-effector position) might be explicitly defined through its direct kinematic model for rigid manipulator, however such a relation for soft manipulator is generally defined in an implicit way through a complex static model (which will be explained in Section 3) for the purpose of modeling soft material deformation.

In the literature, different types of modeling techniques have been proposed to characterize the flexibility of soft robots. Roughly speaking, the PCC (Piece-wise Constant Curvature) modeling approach [13] is broadly employed by the soft robotic community, however the assumption of the constant curvature may

not be always valid, more specifically when external loads are applied on the soft robot. The PCS (Piecewise Constant Strain) model [14], where a finite set of strain vectors describes the soft robot, considers the material proprieties and the geometric non-linearity, which in fact can be seen as an extension of PCC approach. However, like the PCC method, the PCS approach can only be applied to model uniformly slender shapes of soft robots. FEM (Finite Element Method) is suitable to model general geometric form of soft robots [15], and can provide an accurate model for soft robots, but with a relatively higher dimensional model.

In order to estimate the reachable workspace of soft robots with general form, this paper adopts the FEM method to describe the input-output relation of investigated soft robots. In this paper, we solve the problem of workspace estimation for the studied soft robots through 2 steps: firstly the static model used to describe soft robots is deduced by using FEM [16, p. 428], and secondly 2 methods (classical forward method based on Newton iterative approach and novel one based on interval analysis [17]) are proposed to solve the reachable workspace estimation problem for a pre-chosen point of interest. Compared to the classical forward method (which consists of discretizing the actuators' space), the efficiency of the novel approach (named as forward-backward method in this paper) has been validated via different configuration scenarios of soft robots. The preliminary result of this work was presented in the conference [18] and the full version presented in this paper contains new results for FEM static model with external forces, self-contained results on interval analysis, novel uniform spatial grid discretization strategy, detailed algorithm with correct stop condition and comprehensive configuration scenarios of simulation to emphasize the effectiveness of the proposed forward-backward approach.

## 2 Problem Statement

Pick-and-Place operation represents the most basic task that a soft robots' end-effector must be able to perform. But, for such an operation, a soft robot in the first place must be able to reach the position of the object to be handled. In other words, the reachable workspace of the designed structure of the soft robot must include the position of that object, as indicated by the blue point in Fig. 1. Consistently, considering a particular configuration of a soft robot that is controlled via bounded installed actuators (i.e., cables), this paper investigates the evaluation of its reachable workspace.

We would like to emphasize that the cable-driven actuation is only taken as an example in this paper to illustrate the proposed method when estimating the reachable workspace of soft robots, since it is broadly employed in the community of soft robotics. However, since this paper uses the FEM modeling method, and that FEM was applied to different actuation manners, e.g. pneumatic actuation [19] and fluidic actuation [20], therefore the proposed workspace estimation approach is broadly applicable to various types of actuations. In addition, using a different method of actuation will only influence the deduced mathematical FEM model, and the proposed workspace estimation approach remains applicable for other types of actuations.

To tackle the workspace problem, we denote $q_{_E} \in \mathbb{R}^3$ as the displacement vector of the end-effector with respect to its position vector $p_{_E} \in \mathbb{R}^3$. Then, its reachable workspace can be defined as follows:

**Definition 1.** *Consider a soft robot modeled by $\ddot{q} = \Phi(u, q, \dot{q})$, and controlled via installed bounded actuators $u \in \mathcal{U}$, the reachable workspace $\mathcal{W}_{_E}$ of the end-effector $p_{_E} = g(q)$ is a subspace of $\mathbb{R}^3$, that can be defined as:*

$$\mathcal{W}_{_E} = \{p_{_E} \mid \exists u \in \mathcal{U}, q \text{ s.t. } \Phi(u, q, 0) = 0,\ p_{_E} = g(q)\}$$

According to the above definition, the reachable workspace $\mathcal{W}_{_E}$ contains all possible equilibrium positions for which $p_{_E}$ can reach and stay there. We would like to emphasize that the 'stay' property is important and equivalent to the space of all feasible equilibrium points.

Generally speaking, the evaluation of a soft robot's reachable workspace can be physically realized provided that we have the real prototype of the investigated soft robot. But, for the purpose of guiding and optimizing the design of a soft robot before its actual design, it is more reasonable to evaluate its workspace in a virtual environment. To achieve this, two steps are followed: the first one consists of using FEM to establish the mathematical model of soft robots, and the second one consists of estimating the reachable workspace using two different methods.

# 3 Static Model of Soft Robots

In order to estimate the reachable workspace of a soft robot, we need first to deduce the designed soft robot's static model, and for this we adopt the Finite Element Method. This modeling approach firstly consists of spatially discretizing the deformable domain of the structure into smaller finite elements $n_e$, through the creation of a corresponding mesh which contains a finite number of degrees of freedom $n_p$ to interpolate the behavior of the deformable domain by measuring the variation of the associated nodal displacements. In the literature, various geometries are proposed to discretize the spatial domain of a given structure, such as prisms, beams, hexahedrons and tetrahedrons [21, p. 732]. For the purpose of generality and convenience for element matrix integration, this paper selects the linear tetrahedron element as the appropriate meshing structure (Fig. 2 illustrates the implementation of the selected linear tetrahedron mesh on the trunk-like soft robot).

Since we are investigating the reachable workspace of soft robots which contains all equilibrium points, then according to Definition 1, the investigated soft robot's motion [16, p. 428] can be described by the following static model:

$$K_{_N}(q) = H^T(q)u + F(q) \tag{1}$$

where $q \in \mathbb{R}^{3n_p}$ is the nodal displacement vector, $K_{_N}(q) \in \mathbb{R}^{3n_p}$ is the vector of internal forces, $H^T(q) \in \mathbb{R}^{3n_p \times n_u}$ is the direction of the actuators' forces matrix, $u \in \mathbb{R}^{n_u}$ is the control input vector, $n_u$ is the dimension of the input vector, and $F(q) \in \mathbb{R}^{3n_p}$ is the vector of external forces applied to the soft robot.

In the deduced static model (1), the term $u$ represents the applied force to the soft robot which might be generated via different types of actuators. As we have explained before, FEM has been widely used to describe the material deformation subject to different types of actuators, including cable tension [22], cable displacement [22], pneumatic actuation [19], fluidic actuation [20], etc. The only difference is to determine the vector function $H^T(q)$ according to different actuation methods, for the purpose of describing how the associated force $u$ is generated by those actuators (which might be tension, displacement, pressure, etc.), and how $u$ is applied to the soft robot. In this sense, the result presented in this paper is quite general, and is not limited only to cable-driven actuator. We use the cable-driven actuator only as an illustrative example since it is one of the widely used techniques in the community of soft robotics. Also, due to the fact that FEM uses only Newton's second law to describe the robot's motion, therefore only the forces vector can be involved in the final FEM model (1). This explains as well why FEM model contains only the nodes' displacement, but not their rotations.

**Assumption 1.** *The vector of internal forces of the structure $K_{_N}(q)$ can be approximated, in accordance with [16, p. 430], as follows:*

$$K_{_N}(q) = K(q)\, q \tag{2}$$

*where $K(q)$ represents the assembly of each element's stiffness matrix:*

$$K(q) = \sum_{e=1}^{n_e} K_e(q)$$

*and the stiffness matrix [16, p. 429] of an element e is dependent of the elasticity matrix $\nabla$, the strain matrix $B_e(q)$ and the volume $V_e(q)$ of the element e: $K_e(q) = \int_{V_e(q)} B_e^T(q)\, \nabla B_e(q) dv(q)$.*

# 4 Estimation Approaches of Reachable Workspace

In accordance with the workspace definition (see Definition 1), and with Assumption 1 being applied to the static model (1), the workspace of a soft robot can finally be defined by the following set of equations:

$$\begin{aligned} K(q)\, q &= H^T(q)u + F(q) \\ q_{_E} &= Cq \\ p_{_E} &= q_{_E} + p_{_E}^{(0)} \end{aligned} \tag{3}$$

where $q_{_E}$ is the displacement vector of the end-effector with respect to its known initial position vector $p_{_E}^{(0)}$, $p_{_E}$ represents the position vector of the end-effector, and $C$ is a selection matrix associated to the end-effector node coordinates.

Based on the above model, the estimation of the reachable workspace $\mathcal{W}_{_E}$ is then equivalent to determine, for all relevant inputs $u \in \mathcal{U}$, the bound of the end-effector $p_{_E}$ in (3). However, under the FEM framework, the difficulty of such a task lies in the following two reasons: firstly the nonlinearity of $K(q)q$ in (2) and its dependence on material properties, and secondly the lacking of an analytic implicit relation such that $p_{_E} = \phi(u)$, due to the nonlinearity of the mapping $\phi : \mathcal{U} \to \mathcal{W}_{_E}$.

In the following, two different approaches, a forward one and a forward-backward one, will be proposed. Both of them use different numerical schemes to approximate the mapping $\phi$ in order to estimate the reachable workspace $\mathcal{W}_{_E}$ from the bounded input $u \in \mathcal{U}$.

## 4.1 Forward method

The most trivial approach to determine the reachable workspace of a soft robot is to iteratively approximate the map $\phi$ through the discretization of the input bound $\mathcal{U}$ (as illustrated by Fig. 3).

To achieve this, given the information of the end-effector's position vector $p_{_E}^{(j-1)}$ and the vector of nodal displacements $q^{(j-1)}$ (for the case $j = 1$, $p_{_E}^{(0)}$ and $q^{(0)}$ are respectively the initial position of the end-effector and the initial nodal displacement vectors of the investigated soft robot), we apply Newton-Raphson method to obtain the next nodal displacement $q^{(j)}$ corresponding to its input value $u \in \mathcal{U}_d$, with $\mathcal{U}_d$ being the discretized set of $\mathcal{U}$, which can be realized as follows:

$$q^{(j)} = q^{(j-1)} - \Psi_q(u, q^{(j-1)})\ \Psi(u, q^{(j-1)}), \forall u \in \mathcal{U}_d$$

where $\Psi_q(u, q)$ is the gradient of $\Psi(u, q)$ with respect to $q$, and $\Psi(u, q^{(j-1)}) = K(q^{(j-1)})q^{(j-1)} - H^T(q^{(j-1)})u - F(q^{(j-1)})$. Then, the corresponding end-effector position vector can be deduced by:

$$p_{_E}^{(j)} = Cq^{(j)} + p_{_E}^{(0)}$$

Finally, as depicted by Fig. 3, the estimation of the reachable workspace $\mathcal{W}_{_E}$ can be achieved by iterating the above process for all $u \in \mathcal{U}_d$.

In this paper, such an approach is named as the forward method because it is based on using the input vector $u$ to estimate the end-effector's reachable workspace in a forward manner. The computation complexity of this method represents its primary limitation. Since $u \in \mathcal{U} \subset \mathbb{R}^{n_u}$, and suppose that the bound for each entry of $u$ is discretized into $n_d$ subsets, then we will have $n_d^{n_u}$ possible combinations of input for $u$. In this sense, the computation complexity for the forward method will be increased if the number of inputs $n_u$ becomes bigger, and when the discretization precision is increased, it will explode exponentially, even if $n_u$ is small.

We can clearly notice that the dimension of the inputs $n_u$, which may vary depending on various configurations of soft robots, represents the base of this method's computation complexity. However, the end-effector space dimension is invariant, always equal to $\mathbb{R}^3$, and does not depend on the configuration of the investigated soft robot. In accordance with this reflection, it is therefore logical to discretize the end-effector's space with constant dimension, as opposed to discretizing $\mathcal{U}$ with variant dimension, for the purpose of decreasing the computation complexity of the reachable workspace estimation problem. In this paper, we name such a method as the iterative forward-backward method, which will be explained in the following sections.

## 4.2 Forward-Backward method

### 4.2.1 Interval analysis introduction

The proposed forward-backward approach uses interval analysis techniques in order to estimate the workspace of soft robots. Therefore, a brief introduction of the interval analysis techniques is presented in the following. More details can be found in [17].

Consider two real intervals $\mathcal{X}_1 = [\underline{\mathcal{X}}_1, \overline{\mathcal{X}}_1]$ and $\mathcal{X}_2 = [\underline{\mathcal{X}}_2, \overline{\mathcal{X}}_2]$, then according to [17], the product of $\mathcal{X}_1$ and $\mathcal{X}_2$ can be calculated by the following:

$$\mathcal{X}_1\mathcal{X}_2 = \big[min\big(\mathcal{C}(\mathcal{X}_1, \mathcal{X}_2)\big), max\big(\mathcal{C}(\mathcal{X}_1, \mathcal{X}_2)\big)\big]$$

with $\mathcal{C}(\mathcal{X}_1, \mathcal{X}_2) = \{\underline{\mathcal{X}}_1\underline{\mathcal{X}}_2, \underline{\mathcal{X}}_1\overline{\mathcal{X}}_2, \overline{\mathcal{X}}_1\underline{\mathcal{X}}_2, \overline{\mathcal{X}}_1\overline{\mathcal{X}}_2\}$.

The product of a real matrix $M \in \mathbb{R}$ by a real interval $\mathcal{X} = [\underline{\mathcal{X}}, \overline{\mathcal{X}}]$ with appropriate dimension is calculated as follows:

$$M\mathcal{X} = \begin{cases} \left[M\underline{\mathcal{X}}, M\overline{\mathcal{X}}\right], & M > 0 \\ \left[M\overline{\mathcal{X}}, M\underline{\mathcal{X}}\right], & M < 0 \end{cases}$$

However, due to the wrapping effect ( $A\mathcal{X} \supset \{Ax \mid x \in \mathcal{X}\}$ ) [17], this technique leads to an over-estimation of the resulted space which can be explained by considering the following example:

$$A = \begin{pmatrix} 1 & 1 \\ 0 & 1 \end{pmatrix},\ \mathcal{X} = \begin{pmatrix} [-1, 0] \\ [1, 2] \end{pmatrix}$$

then

$$A\mathcal{X} = \begin{pmatrix} [0, 2] \\ [1, 2] \end{pmatrix}$$

which implies that $(0, 2)^T$ belongs to $A\mathcal{X}$, whereas it does not belong to the actual value set $\mathbb{B} = \{Ax \mid x \in \mathcal{X}\}$, as illustrated by Fig. 4.

Therefore, we need to eliminate the resulted over-estimation in order to obtain the true space, and this will be implemented in the proposed forward-backward approach and explained in the following.

#### 4.2.2 Forward-Backward approach introduction

In what follows, we present a brief overview of how the proposed forward-backward approach operates.

On the opposite to the forward approach which consists of discretizing the bounded input space, the forward-backward approach is based on the idea of discretizing the end-effector's space which is always constant, typically 3 (the dimension of position) or 6 (with orientation), regardless of how many actuators are installed. However, the process of discretization of the end-effector's space requires firstly the knowledge of its bound. For this, we estimate this boundary, at the $(j-1)$th iteration, via a linear approximation between the corresponding displacement vector $q$ and the input vector $u$:

$$K(q^{(j-1)})\delta q^{(j)} = H^T(q^{(j-1)})\delta u^{(j-1)} + F(q^{(j-1)})$$

with $\delta q_{E}^{(j)} = C\delta q^{(j)}$, $p_{E}^{(j)} = \delta q_{E}^{(j)} + p_{E}^{(j-1)}$, and

$$\begin{aligned} \delta q^{(j)} &= q - q^{(j-1)} \\ \delta u^{(j-1)} &= u - u^{(j-1)} \end{aligned}$$

where $\delta q^{(j)}$ and $\delta u^{(j-1)}$ represent respectively the displacement vector and the input vector with reference to the prior soft robot configuration.

Roughly speaking, based on the above approximation, we firstly implement interval analysis techniques in order to forwardly estimate the end-effector's workspace $\mathcal{W}_{E}^{(j)}$ for the related $\delta q^{(j)}$ (as illustrated by Step 1 in Fig. 5). Secondly, since we now have the information of the workspace $\mathcal{W}_{E}^{(j)} \subset \mathbb{R}^3$, then we adopt a prescribed precision to discretize it. After that, we use the current end-effector's position $p_{E}^{(j-1)}$ as a base to determine a feasible small displacement neighborhood around it (noted as $\mathcal{W}_{E_s}^{(j)}$ in Step 2 of Fig. 5). Thirdly, in order to guarantee that the robot can reach this feasible small displacement neighborhood $\mathcal{W}_{E_s}^{(j)}$, we backwardly calculate the equivalent input vector $u^{(j)}$ (as depicted in the domain $\mathcal{U}$ in Step 3 of Fig. 5). In the fourth step of the method, we calculate the new input bound $\mathcal{U}^{(j)}$ using the deduced value of $u^{(j)}$ (illustrated as Step 4 in Fig. 5). Next, based on the obtained value of $\mathcal{U}^{(j)}$, we can forwardly compute the end-effector's new bound $\mathcal{W}_{E}^{(j+1)}$. If $\mathcal{W}_{E_s}^{(j)}$ and $\mathcal{W}_{E}^{(j+1)}$ both contain the feasible small displacement neighborhood of the end-effector, it implies that this neighborhood has already been visited. Such a conclusion allows us to efficiently and accurately shrink the over-estimated workspace caused by interval analysis (see Section 5 for the details). Finally, the proposed approach can explore the whole reachable workspace $\mathcal{W}_{E}$ by iterating the above procedure.

In comparison with the forward approach, the forward-backward method provides the following two benefits:

1. Since the end-effector space is fixed to 3 for the position case, the forward-backward approach can significantly decrease the dimension of the discretized space in the forward method;

2. The forward approach cannot reduce the number of iterations, whereas, when discretizing the end-effector's space using a specified precision (with $n_d$ sub-spaces), the forward-backward method can eliminate the wrong sub-spaces caused by the interval estimation technique.

# 5 Forward-Backward method Realization

In this section, we present the details of how the forward-backward method is realized (refer to Fig. 5).

### Step 1: Forward Over-estimation of $\mathcal{W}_E^{(j)}$ using interval analysis

In the first step of the forward-backward approach, interval analysis techniques are used for the purpose of forwardly estimating the end-effector's workspace. To do this, we firstly need to linearly approximate the workspace defined by (3) with the knowledge of the end-effector's position $p_E^{(j-1)}$, of the displacement vector $q^{(j-1)}$, and of the corresponding input vector $u^{(j-1)} \in \mathcal{U}^{(j-1)}$, as follows:

$$\begin{aligned} K(q^{(j-1)})\delta q^{(j)} &= H^T(q^{(j-1)})\delta u^{(j-1)} + F(q^{(j-1)}) \\ \delta q_E^{(j)} &= C\delta q^{(j)} \\ p_E^{(j)} &= \delta q_E^{(j)} + p_E^{(j-1)} \end{aligned} \tag{4}$$

with

$$\delta q^{(j)} = q - q^{(j-1)}$$

and

$$\delta u^{(j-1)} = u - u^{(j-1)}$$

Next, suppose that the actuators are well installed in a manner that the investigated soft robot is always controllable [23], then the matrix $K(q^{(j-1)})$ is always invertible for any given value $q^{(j-1)}$. Let us now introduce the matrix $A$ as:

$$A(q^{(j-1)}) = CK^{-1}(q^{(j-1)})H^T(q^{(j-1)})$$

and define the matrix $A^+$ by

$$A^+ = \max\{0, A\}$$

where the operation $\max\{\cdot\}$ is applied element-wise [24], and

$$A^- = A - A^+$$

With the above necessary elements, for the related displacement $\delta q^{(j)}$, the over-estimated workspace $\mathcal{W}_E^{(j)}$ corresponding to the input bound $\mathcal{U}^{(j-1)}$ can be calculated via the following theorem:

**Theorem 1.** *Given a soft robot's controllable configuration, with the input bound $\mathcal{U}^{(j-1)}$ defined as*

$$\mathcal{U}^{(j-1)} = [\underline{\delta u}^{(j-1)}, \overline{\delta u}^{(j-1)}]$$

*then the end-effector workspace $\mathcal{W}_E^{(j)}$ is over-estimated as*

$$\mathcal{W}_E^{(j)} = \left\{ p_E^{(j)} \in \mathbb{R}^3 | p_E^{(j)} \in \left[ \underline{p}_E^{(j)}, \overline{p}_E^{(j)} \right] \right\} \tag{5}$$

*with*

$$\underline{p}_E^{(j)} = A^+\underline{\delta u}^{(j-1)} + A^-\overline{\delta u}^{(j-1)} + CK^{-1}(q^{(j-1)})F(q^{(j-1)}) + p_E^{(j-1)}$$

*and*

$$\overline{p}_E^{(j)} = A^+\overline{\delta u}^{(j-1)} + A^-\underline{\delta u}^{(j-1)} + CK^{-1}(q^{(j-1)})F(q^{(j-1)}) + p_E^{(j-1)}.$$

*Proof.* Using the linear approximation defined in (4), the nodal displacement vector can be directly deduced as:

$$\delta q^{(j)} = K^{-1}(q^{(j-1)})\big[H^T(q^{(j-1)})\delta u^{(j-1)} + F(q^{(j-1)})\big]$$

With the defined matrix $A$, we can then use the above equation to write the end-effector displacement in function of the matrix $A$, which yields:

$$\begin{aligned} p_{_E}^{(j)} &= C\delta q^{(j)} + p_{_E}^{(j-1)} \\ &= CK^{-1}(q^{(j-1)})\big[H^T(q^{(j-1)})\delta u^{(j-1)} + F(q^{(j-1)})\big] + p_{_E}^{(j-1)} \\ &= CK^{-1}(q^{(j-1)})H^T(q^{(j-1)})\delta u^{(j-1)} + CK^{-1}(q^{(j-1)})F(q^{(j-1)}) + p_{_E}^{(j-1)} \\ &= A(q^{(j-1)})\delta u^{(j-1)} + CK^{-1}(q^{(j-1)})F(q^{(j-1)}) + p_{_E}^{(j-1)} \end{aligned}$$

Next, according to Lemma 3 in [24], the following over-estimation is obtained:

$$A^+\underline{\delta u}^{(j-1)} + A^-\overline{\delta u}^{(j-1)} \leq A\delta u \leq A^+\overline{\delta u}^{(j-1)} + A^-\underline{\delta u}^{(j-1)}$$

By simply defining

$$\underline{p}_{_E}^{(j)} = A^+\underline{\delta u}^{(j-1)} + A^-\overline{\delta u}^{(j-1)} + CK^{-1}(q^{(j-1)})F(q^{(j-1)}) + p_{_E}^{(j-1)}$$

and

$$\overline{p}_{_E}^{(j)} = A^+\overline{\delta u}^{(j-1)} + A^-\underline{\delta u}^{(j-1)} + CK^{-1}(q^{(j-1)})F(q^{(j-1)}) + p_{_E}^{(j-1)}$$

that leads to:

$$\underline{p}_{_E}^{(j)} \leq p_{_E}^{(j)} \leq \overline{p}_{_E}^{(j)}$$

Finally, we obtain the over-estimated workspace $\mathcal{W}_{_E}^{(j)}$ defined by (5). □

## Step 2: Feasible small displacement neighborhood $\mathcal{W}_{_{E_s}}^{(j)}$ computation

The purpose of the second step consists of determining the feasible small displacement neighborhood $\mathcal{W}_{_{E_s}}^{(j)}$ around the current end-effector position $p_{_E}^{(j-1)}$.

To do this, we propose two strategies to discretize the over-estimated workspace $\mathcal{W}_{_E}^{(j)}$ calculated via Step 1 with a specified precision to obtain a related discretized space $\mathcal{W}_{_{E_d}}^{(j)}$. The first discretization strategy is based on the principle that linear approximations in the FEM model are only valid within $\pm 5\%$ of the displacement, thus the first strategy consists of using the linear approximation of $K_{_N}(q)$ for varying the value of $p_{_E}^{(j-1)}$ in each of the three Cartesian directions ($x$, $y$ and $z$) with a ratio of $\pm 5\%$. Denote

$$l^{(j-1)} = \|p_{_E}^{(j-1)}\|_2$$

which represents the Euclidean distance between $p_{_E}^{(j-1)}$ and the origin of the earth frame, then such a scheme enables us to obtain the following discretized space $\mathcal{W}_{_{E_d}}^{(j)}$:

$$\mathcal{W}_{_{E_d}}^{(j)} = \Big\{p_{_E}^{(j)} \in \mathcal{W}_{_E}^{(j)} | p_{_E}^{(j)} = p_{_E}^{(j-1)} + 5\% l^{(j-1)}\Gamma, \text{ for } \Gamma \in \mathbb{Z}^3\Big\} \tag{6}$$

The second discretization strategy is simpler and it consists of discretizing the space $\mathcal{W}_{_{E_d}}^{(j)}$ by using a globally uniform spatial grid with a globally small pre-defined precision $s_{E_d}$, i.e.,

$$\mathcal{W}_{_{E_d}}^{(j)} = \Big\{p_{_E}^{(j)} \in \mathcal{W}_{_E}^{(j)} | p_{_E}^{(j)} = p_{_E}^{(j-1)} + s_{E_d}\Gamma, \text{ for } \Gamma \in \mathbb{Z}^3\Big\}$$

In addition, at the point $p_{_E}^{(j-1)}$, we can define its $\eta$-neighborhood as

$$\mathcal{S}_\eta(p_{_E}^{(j-1)}) = \Big\{\tilde{p}_{_E} \in \mathbb{R}^3 | \|p_{_E}^{(j)} - p_{_E}^{(j-1)}\|_\infty = \eta\Big\}$$

where $\eta$ is equal either to $5\% l^{(j-1)}$ or $s_{E_d}$, depending on the chosen discretization strategy. Consequently, we can finally deduce the feasible small neighborhood around $p_{_E}^{(j-1)}$ as follows:

$$\mathcal{W}_{_{E_s}}^{(j)} = \mathcal{W}_{_{E_d}}^{(j)} \cap \mathcal{S}_\eta(p_{_E}^{(j-1)}) \tag{7}$$

The illustration presented by Fig. 6 clearly depicts the relation between $\mathcal{W}_{_E}^{(j)}$, the discretization of its space $\mathcal{W}_{_{E_d}}^{(j)}$, and the relative feasible small displacement neighborhood space $\mathcal{W}_{_{E_s}}^{(j)}$.

### Step 3: Backward configuration estimation

After having calculated the feasible small neighborhood $\mathcal{W}_{E_s}^{(j)}$ via (7), the third step consists of computing the feasible input vector $u^{(j)}$ via a backward mechanism, to guarantee that any point $\hat{p}_E^{(j)} \in \mathcal{W}_{E_s}^{(j)} \setminus p_E^{(j-1)}$ might be accessible by the end-effector of the soft robot (see Fig. 7).

For this, with the values of $p_E^{(j-1)}$ and $q^{(j-1)}$, the associated deformation vector of the end-effector can be then calculated as:

$$\hat{q}_E^{(j)} = \hat{p}_E^{(j)} - p_E^{(j-1)}$$

Consequently we can calculate the equivalent input and displacement vector by solving the optimization problem formulated below:

$$\begin{aligned} [u^{(j)}, q^{(j)}] = \min_{u,q} \quad & \|q_E - \hat{q}_E^{(j)}\|_2^2 \\ \text{s.t.} \quad & u \in \mathcal{U} \\ & K(q)q = H^T(q)u + F(q) \\ & q_E = Cq \end{aligned} \tag{8}$$

Solving the backward mechanism (8) yields the feasible input vector $u^{(j)}$ with its related feasible displacement vector $q^{(j)}$, which will eventually drive the soft robot's end-effector to reach $\hat{p}_E^{(j)}$.

Finally, we deduce the end-effector position associated with the optimal displacement vector $q^{(j)}$ as

$$p_E^{(j)} = Cq^{(j)} + p_E^{(j-1)}.$$

It is important to state that, for each iteration $(j)$, the inverse problem (8) has a unique solution, because this optimization problem is formulated inside a small neighborhood of $\hat{q}_E^{(j)}$, and we always solve this problem with reference to the prior iteration $(j-1)$.

### Step 4: Update input bound $\mathcal{U}^{(j)}$

In the fourth step of the forward-backward approach, with the information of $\mathcal{U}^{(j-1)}$, we calculate the new input bound $\mathcal{U}^{(j)}$ related to the input vector $u^{(j)}$ obtained in the third step.

To this aim, let us define the following diagonal $n_u \times n_u$ matrix:

$$\text{diag}(u^{(j)}) = \text{diag}\left\{u_1^{(j)}, \cdots, u_{n_u}^{(j)}\right\}$$

where $u_i^{(j)}$ $(1 \leq i \leq n_u)$ represents the $i$th related value of $u^{(j)}$, then the new input bound can be updated by the following equation:

$$\mathcal{U}^{(j)} = \mathcal{U}^{(j-1)} - \text{diag}(u^{(j)}) \times \mathbf{1}_{n_u \times 2} \tag{9}$$

with $\mathbf{1}_{n_u \times 2}$ being an $n_u \times 2$ dimensional matrix whose entries are equal to 1. The presented updating scheme is illustrated in Fig. 8.

### Step 5: Condition of stop/iteration

After having obtained $p_E^{(j-1)}$, $q^{(j-1)}$, $u^{(j-1)}$ and $\mathcal{U}^{(j-1)}$, by applying the above presented forward-backward method, we might get $p_E^{(j)}$, $q^{(j)}$, $u^{(j)}$ and $\mathcal{U}^{(j)}$. Iteratively, we can finally obtain the whole reachable workspace of the pre-chosen point of interest.

For a particular configuration $p_E^{(j-1)}$, assume that the corresponding over-estimated workspace $\mathcal{W}_E^{(j)}$ has been calculated via Step 1, then its related discretized space $\mathcal{W}_{E_d}^{(j)}$ can be computed via Step 2, from which, according to (7), an associated feasible small displacement neighborhood $\mathcal{W}_{E_s}^{(j)}$ is deduced. An important property of Step 2 is that it allows us to eliminate certain non-feasible neighborhoods around $p_E^{(j-1)}$, which results in decreasing the amount of the feasible small displacement neighborhoods $\mathcal{W}_{E_s}^{(j)}$ to be explored for the next iteration of the forward-backward approach, as illustrated in Fig. 6 by verifying the condition (7). On the other hand, given the information of $\mathcal{W}_{E_s}^{(j-1)}$ and the newly calculated feasible small displacement neighborhood $\mathcal{W}_{E_s}^{(j)}$ from (7), an additional property which allows us to further shrink the space to be explored

is that some of the points belonging to $\mathcal{W}_{E_s}^{(j)}$ would probably have been explored by the former iterations, noted as $\mathcal{W}_{E_\cup}^{(j-1)}$ where

$$\mathcal{W}_{E_\cup}^{(j-1)} = \cup_{k=1}^{j-1} \mathcal{W}_{E_s}^{(k)}$$

The above elimination procedure is effectuated in Step 5, as depicted in Fig. 9, by verifying the following condition:

$$\mathcal{W}_{E_s}^{(j)} \leftarrow \mathcal{S}_\eta(p_E^{(j-1)}) \setminus (\mathcal{W}_{E_\cup}^{(j-1)} \cap \mathcal{S}_\eta(p_E^{(j-1)})) \tag{10}$$

Combining these two conditions (eq. (7) in Step 2 and eq. (10) in Step 5) allows us to shrink the space to be explored efficiently and accurately, which will result in significantly reducing the computation complexity of the proposed forward-backward approach (as shown in the simulation results Section 6).

Obviously, for any given point $\tilde{p}_E$ belonging to the union of the $j$th iteration, i.e., $\tilde{p}_E \in \mathcal{W}_{E_s}^{(j)}$, if the corresponding end-effector position $\tilde{p}_E^{(j)}$ belongs to the union of the $(j-1)$th iteration (as shown in Fig. 10), i.e., $\tilde{p}_E \in \mathcal{W}_{E_\cup}^{(j-1)}$, then we can draw the conclusion that the neighborhood $\tilde{p}_E^{(j)}$ has already been visited. The above observation can be expressed as the following check-condition:

$$\exists j \in \mathbb{N}, \text{ s.t. } \tilde{p}_E \in \mathcal{W}_{E_\cup}^{(j-1)}, \ \ \forall \tilde{p}_E \in \mathcal{W}_{E_s}^{(j)}$$

or equivalently

$$\exists j \in \mathbb{N}, \text{ s.t. } \mathcal{W}_{E_\cup}^{(j)} = \mathcal{W}_{E_\cup}^{(j-1)}$$

Consequently, we deduce that all feasible small displacement neighborhoods were explored. At this level, we can obtain the end-effector's reachable workspace via the following equation:

$$\mathcal{W}_E = \mathcal{W}_{E_\cup}^{(j-1)}.$$

### Realization of the algorithm

In the table below, a brief algorithm is presented in order to describe the main steps of the forward-backward approach.

**Algorithm 1** Calculate $\{p_E, q, u, \mathcal{U}, \mathcal{W}_{E_s}, \mathcal{W}_{E_\cup}\}^{(j)}, \mathcal{W}_E$

**Require:** $\Gamma, s_{E_d}, \{p_E, q, u, \mathcal{U}, \mathcal{W}_{E_s}, \mathcal{W}_{E_\cup}\}^{(j-1)}$
  **while** $\mathcal{W}_{E_s}^{(j)} \notin \mathcal{W}_{E_\cup}^{(j-1)}$ **do** ▷ Stop Condition.
    $\mathcal{W}_E^{(j)} \leftarrow f_1(\{p_E, q, \mathcal{U}\}^{(j-1)})$ ▷ Step 1: Forward estimation of $\mathcal{W}_E^{(j)}$, eq. (5)
    $\mathcal{W}_{E_d}^{(j)} \leftarrow f_2(p_E^{(j-1)}, \Gamma, s_{E_d})$ ▷ Step 2: Discretized space $\mathcal{W}_{E_d}^{(j)}$, eq. (6)
    $\mathcal{W}_{E_s}^{(j)} \leftarrow \mathcal{W}_{E_d}^{(j)} \cap \mathcal{S}_\eta(p_E^{(j-1)})$ ▷ Step 2: Feasible small displacement neighborhood $\mathcal{W}_{E_s}^{(j)}$, eq. (7)
    $\hat{p}_E^{(j)} \leftarrow \mathcal{W}_{E_s}^{(j)} \setminus p_E^{(j-1)}$ ▷ Exclusion.
    $\hat{q}_E^{(j)} \leftarrow \hat{p}_E^{(j)} - p_E^{(j-1)}$
    $\{p_E, q, u\}^{(j)} \leftarrow f_3(\hat{q}_E^{(j)}, q^{(j-1)})$ ▷ Step 3: Backward estimation of $u^{(j)}$, eq. (8)
    $\mathcal{U}^{(j)} \leftarrow f_4(u^{(j)}, \mathcal{U}^{(j-1)})$ ▷ Step 4: New input bound $\mathcal{U}^{(j)}$, eq. (9)
    $\mathcal{W}_{E_s}^{(j)} \leftarrow \mathcal{S}_\eta(p_E^{(j-1)}) \setminus (\mathcal{W}_{E_\cup}^{(j-1)} \cap \mathcal{S}_\eta(p_E^{(j-1)}))$ ▷ Step 5: Dismiss explored feasible neighborhood, eq. (10)
    $\mathcal{W}_{E_\cup}^{(j)} \leftarrow \mathcal{W}_{E_\cup}^{(j-1)} \cup \mathcal{W}_{E_s}^{(j)}$ ▷ Append.
    $\{p_E, q, u, \mathcal{U}, \mathcal{W}_{E_\cup}\}^{(j-1)} \leftarrow \{p_E, q, u, \mathcal{U}, \mathcal{W}_{E_\cup}\}^{(j)}$ ▷ Update Values.
    $j \leftarrow j + 1$ ▷ Next iteration.
  **end while**
  $\mathcal{W}_E \leftarrow \mathcal{W}_{E_\cup}^{(j-1)}$ ▷ The Estimated Reachable Workspace.

## 6 Comprehensive Simulation Results

This section presents the comparative results between the forward and forward-backward approaches for 3 different configuration scenarios for a trunk-like soft robot with a Young's modulus $E = 1.8 \times 10^7 Pa$, and a

Poisson ratio $\nu = 0.45$. The simulations were implemented on an Intel Xeon(R) with a 16-GB RAM and a 3.50 GHz processor.

We consider those different scenarios where the trunk-like soft robot is actuated by different cable routing configurations, then we implement both the forward and forward-backward approach in order to estimate the reachable workspace $\mathcal{W}_{_E}$ for each scenario. The results of both approaches are then superposed and illustrated by three-view drawing ($Oxy$, $Ozy$, and $Ozx$ plans) for each scenario. For the forward approach, we propose to discretize the actuation force vector with a discretization step size of 1 Newton(unit) in order to respect the linear approximation of the FEM model and ensure small displacements.

## 6.1 Scenario 1: Trunk-like soft robot actuated by two cables.

In the first scenario, we consider a cable routing configuration where the trunk-like soft robot is actuated by two cables (as shown by Fig. 11a). The applied force is of the following range: $\mathcal{U}^{(0)} = \mathcal{U} = [0\ 100] \times [0\ 100]$.

Following the procedure presented in Section 4.1, we firstly apply the forward approach with a discretization number equal $n_d = 100$, and we obtain the corresponding estimation of $\mathcal{W}_{_E}$ ( illustrated by blue colored points in Figs. 11b, 11c and 11d) for this soft robot's configuration. In term of operations' computation complexity, the forward approach requires $n_d^{n_u} = 100^2$ operations, and in term of time's computation complexity, it took approximately 1463 seconds to obtain the full estimation of this scenario workspace.

Next, we apply the proposed forward-backward interval analysis approach by following the procedure presented in Section 5. Given the value of $\mathcal{U}^{(0)}$ we forwardly estimate $\mathcal{W}_{_E}^{(1)}$ using in Step. 1 of Fig. 5, next, we calculate a feasible small displacement neighborhood $\mathcal{W}_{_{E_s}}^{(1)}$ as indicated in Step. 2 of Fig. 5. After, as explained in Step. 3 of Fig. 5, we use the backward mechanism to compute the feasible input vector $u^{(1)}$ of each configuration belonging to $\mathcal{W}_{_{E_s}}^{(1)}$. Finally, we compute $\mathcal{U}^{(1)}$ as shown in Step. 4 of Fig. 5. We iterate the above process for the next iterations until the stop condition is verified, as explained in Step. 5 and illustrated by Fig. 10.

For this scenario, the forward-backward approach took 37 complete iterations and found a total of 635 feasible points in the workspace with a computation time of 757 seconds. Those obtained feasible points are depicted by red colored points in Figs. 11b, 11c and 11d, and the union of all small neighborhood of those feasible points gives the estimation of workspace $\mathcal{W}_{_E}$, which is represented by the gray zone with green contour. It is clear to see from the three-view drawing that the workspace estimation result obtained via forward-backward method coincides with that obtained via forward approach.

Moreover, for a complete 37 iterations it is expected to have $\mathcal{W}_{_{E_d}} = 6^{37} = 6.18 \times 10^{28}$ points to explore. However, what we actually explored is a total of $\mathcal{W}_{_{E_d}} = 1680$ points, and a final total of $\mathcal{W}_{_{E_s}} = 635$ feasible points. This significant reduction was partially due to the elimination process of inappropriate configurations from Step. 2 (See Fig. 6), but mainly due to the elimination of all feasible configurations that were already explored during Step. 5 (See Fig. 9).

Consequently, the proposed forward-backward approach can yield comparable workspace estimation precision compared to forward method, and at the same time reduce both the number of operations and the computational time required for the workspace estimation of this soft robot's configuration.

## 6.2 Scenario 2: Trunk-like soft robot actuated by three cables.

In this scenario, we consider a cable routing configuration where the trunk-like soft robot is actuated by three cables (as shown by Fig. 12a). The applied force is of the following range: $\mathcal{U}^{(0)} = \mathcal{U} = [0\ 100] \times [0\ 100] \times [0\ 150]$.

First, we apply the forward approach with a discretization precision of $n_d = 100$, and we achieve the following workspace $\mathcal{W}_{_E}$ estimation (illustrated by blue colored points in Figs. 12b, 12c, and 12d) of this particular configuration. In term of operations' computation complexity, the forward approach requires $n_d^{n_u} = 100^3$ operations, and in term of time's computation complexity, it will approximately require $1.46 \times 10^5$ seconds to obtain the full estimation of this scenario workspace.

Next, we apply the forward-backward interval analysis approach using the equations presented in Section 5. For this scenario, the forward-backward approach took 44 complete iterations and calculated a total of 1941 feasible points in the workspace with a computation time of 2063 seconds. Those achieved feasible points are illustrated with red colored points in Figs. 12b, 12c and 12d, and the union of all small neighborhood

of those feasible points yield the estimated workspace $\mathcal{W}_{E}$, which is represented by the gray zone within the green contour. Using the three-view illustration, we can clearly observe that the estimated workspace calculated via the proposed forward-backward approach conforms with that obtained through the forward approach.

Furthermore, for a complete 44 iterations it is expected to get $\mathcal{W}_{E_d} = 6^{44} = 1.17 \times 10^{34}$ points to investigate. Yet, the total of points that we actually explored is $\mathcal{W}_{E_d} = 5466$, with a final total of $\mathcal{W}_{E_s} = 1941$ feasible points. This substantial reduction was slightly due to Step. 2 (refer to Fig. 6) elimination process of irrelevant configurations, but considerably due to the exclusion of already explored feasible configurations throughout Step. 5 (See Fig. 9).

Subsequently, the proposed forward-backward approach can achieve comparable workspace estimation precision compared to the forward method, and simultaneously reduce both the number of operations and the computational time required for the workspace estimation of this soft robot's configuration.

### 6.3 Scenario 3: Trunk-like soft robot actuated by four cables.

In this scenario, we consider a cable routing configuration where the trunk-like soft robot is actuated by four cables (as shown by Fig. 13a). The applied force is of the following range: $\mathcal{U}^{(0)} = \mathcal{U} = [0\ 100] \times [0\ 100] \times [0\ 150] \times [0\ 150]$.

First, we apply the forward approach with a discretization precision equal $n_d = 100$, and we obtain the corresponding estimation of $\mathcal{W}_{E}$ (illustrated by blue colored points in Figs. 13b, 13c and 13d) for this soft robot's configuration. In term of operations' computation complexity, the forward approach requires $n_d^{n_u} = 100^4$ operations, and in term of time's computation complexity, it will approximately take $1.46 \times 10^7$ seconds to achieve the full estimation of this scenario workspace.

Next, we apply the proposed forward-backward interval analysis approach by following the procedure presented in Section 5. For this scenario, the forward-backward approach took 42 complete iterations and computed a total 3667 feasible points in the workspace with a computation time of 3733 seconds. Those obtained feasible points are depicted by red colored points in Figs. 13b, 13c and 13d, and the union of all small neighborhood of those feasible points gives the estimation of the workspace $\mathcal{W}_{E}$, which is represented by the gray zone with green contour. It is clear to see from the three-view drawing that the workspace estimation result obtained via forward-backward method coincides with that obtained via forward approach.

In addition, for a complete 42 iterations it is expected to have $\mathcal{W}_{E_d} = 6^{42} = 4.81 \times 10^{32}$ points to explore. However, what we actually explored is a total of $\mathcal{W}_{E_d} = 10626$ points, and a final total of $\mathcal{W}_{E_s} = 3667$ feasible points. This significant reduction was partially due to the elimination process of inappropriate configurations from Step. 2 (See Fig. 6), but mainly due to the elimination of all feasible configurations that were already explored during Step. 5 (See Fig. 9). Based on those results, the same conclusion can be drawn, i.e., the proposed forward-backward approach can yield comparable workspace estimation precision compared to forward method, and at the same time reduce both the number of operations and the computational time required for the workspace estimation of this soft robot's configuration.

### 6.4 Notes on Computation Complexity

For each particular soft robot's configuration, we compared the workspace estimation results obtained via the forward and forward-backward approach. According to the simulation results, we observe that the proposed forward-backward approach has, compared to the forward approach, significantly reduced the computation complexity in both operations and time of the workspace estimation of soft robots.

In the following table (see Table 1), we recapitulate the operations and time computation complexity of each scenario, where the computation complexity of the forward approach for both the second and the third scenario is just approximated since they required a very large time.

Visually, both the operations and time computation complexity can be illustrated respectively by Fig. 14a and Fig. 14b, where we can clearly observe the influence of increasing the inputs' dimension on the forward approach which makes the computation complexity explodes exponentially in both operations and time, whereas the computation complexity of the proposed forward-backward approach remains almost linearly stable.

# 7 Discussion and Perspectives

In this paper, we proposed a forward-backward approach, based on interval analysis, to efficiently estimate the workspace of soft robots. Our approach uses FEM (3) as the modeling method, where the nodal displacement of elements $q$ is used to describe the deformation of material. As a consequence, such an approach cannot directly catch the orientation information of the end-effector, and that is the reason why this paper discusses only the workspace of the end-effector's position $p_{_E}$ in (3), by selecting $C \in \mathbb{R}^{3\times 3n_p}$ as a selection associated to the end-effector node coordinates.

However, we would like to emphasize that such an approach might be adapted to analyze the orientation workspace of the end-effector by simply modifying the above matrix $C$. Precisely, denote $q_{_{E_1}}, q_{_{E_2}}$ and $q_{_{E_3}}$ as 3 independent nodal positions around the end-effector, which can be used to define a unique plane of the end-effector. Then, we can always properly choose the matrix $C \in \mathbb{R}^{6\times 3n_p}$ such that $q_{_E}$ now is a function of those 3 points and contains both position and orientation information of the defined plane. It is evident that such a modification of matrix $C$ will not influence the proposed approach to estimate the workspace of soft robots, since what we need to do is to adapt the matrix $C$ in the workspace set (3).

In addition, the physical buckling phenomenon can occur under special combined action of cables with certain tensions, i.e., under special configuration with specific applied inputs. In other words, buckling phenomenon might not happen if the used numerical method can avoid those special configurations when calculating the workspace. In general, for the classical forward method, this phenomenon might occur which however might be avoided in the proposed forward-backward method, due to the backward mechanism (Step 3) applied to the feasible small displacement neighborhood around the current configuration (Step 2). Precisely, suppose that the current configuration (note the combined cable tension as $u_B$, the nodal displacement as $q_B$, and the end-effector position as $p_B$) is quite close to yield buckling. The proposed forward-backward method will firstly determine a feasible small displacement neighborhood around $p_B$ (Step 2), based on which it will backwardly calculate the associated actuation action around $u_B$ which can lead the end-effector of the soft robot to reach the points in the determined feasible small displacement neighborhood. In other words, since those equilibrium points are all located inside this small neighborhood, i.e., there exist feasible paths to link those points, thus the proposed forward-backward approach can always assess the workspace under this situation, even if it is quite close to buckling. This can be seen as another advantage of the proposed forward-backward method, compared to the classical forward one.

# 8 Conclusions

Using the FEM modeling approach, we have presented a classic method, namely the forward approach, which consists of discretizing the actuators' space in order to achieve the reachable workspace estimation of soft robots. In order to reduce the computation complexity of this forward method, we have proposed a novel method, named as the forward-backward approach, which consists of discretizing the end-effector's space in order to achieve an efficient estimation of the reachable workspace of soft robots.

The proposed approach was validated via various soft robot's configurations by using the forward method as a comparative reference. Through those simulations, we have shown the efficiency of the proposed forward-backward method in reducing the complexity of both operations and time required to achieve the full estimation of the reachable workspace of soft robots, comparing to the basic forward method which explodes exponentially when the actuator's dimension increases.

# 9 Figures

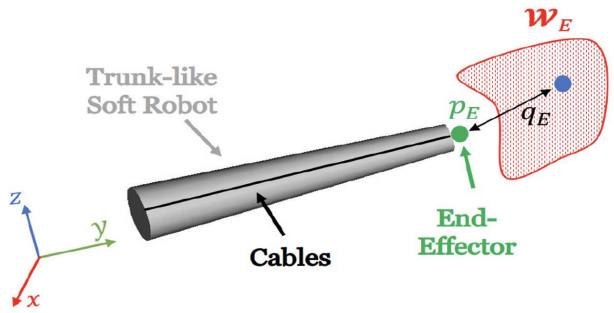


Figure 1: Scheme of the investigated soft robot.

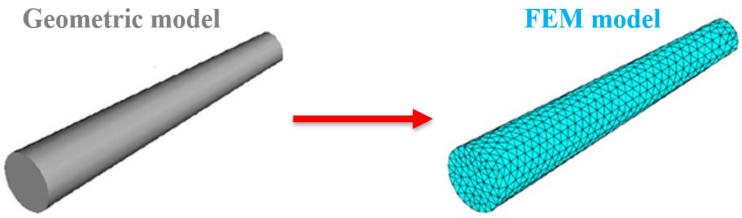


Figure 2: Geometric model and the related FEM model.

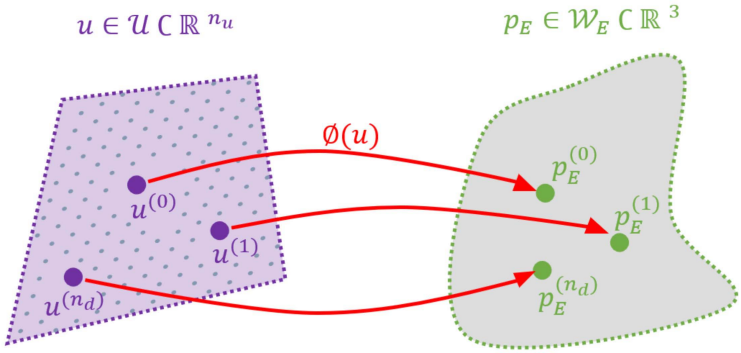


Figure 3: Newton method based forward approach.

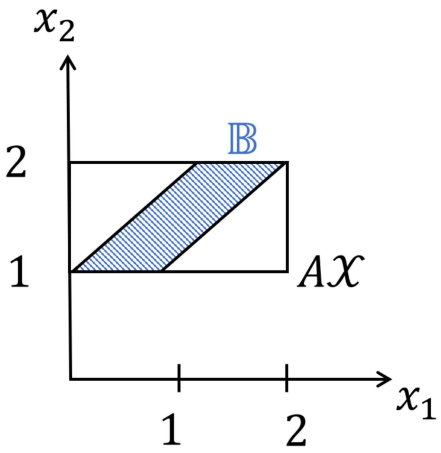


Figure 4: Over-estimation introduced by the wrapping effect.

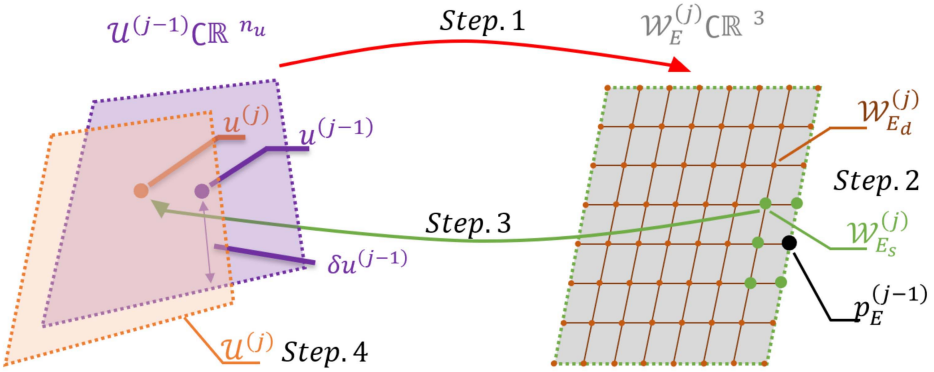


Figure 5: Interval analysis based forward-backward method.

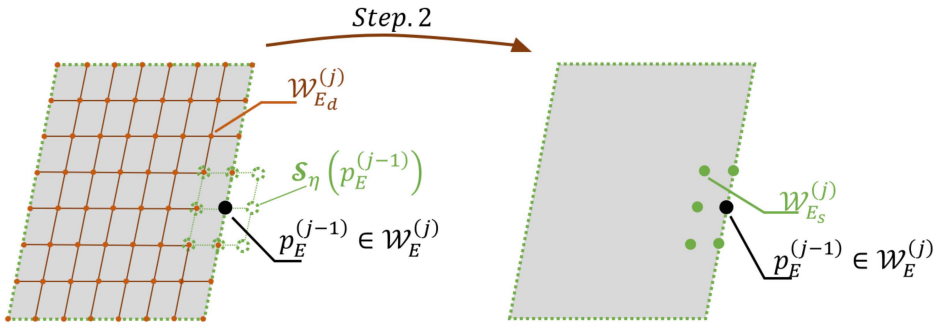


Figure 6: Elimination of non-feasible neighborhoods.

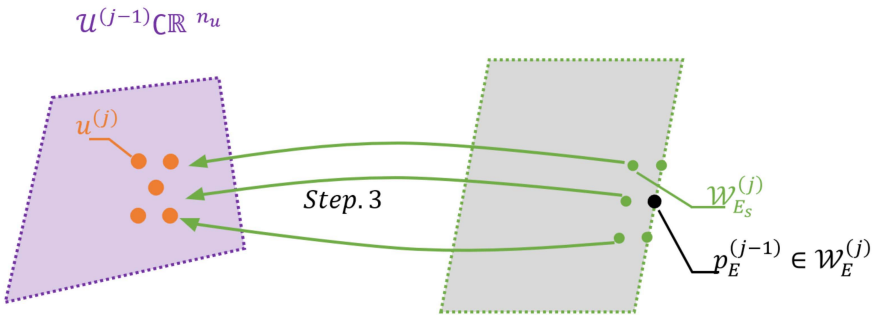


Figure 7: Estimation of input $u^{(j)}$.

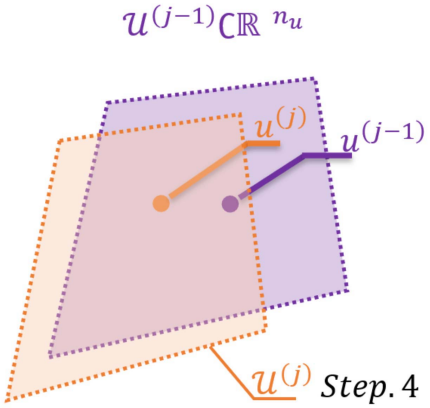


Figure 8: Update the boundedness of input $\mathcal{U}^{(j)}$.

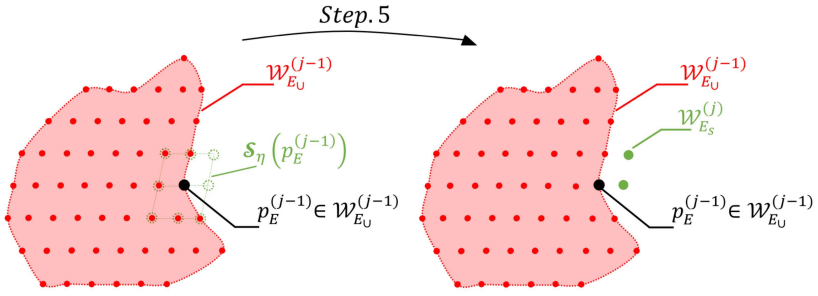


Figure 9: Dismiss pre-explored feasible displacement neighborhoods.

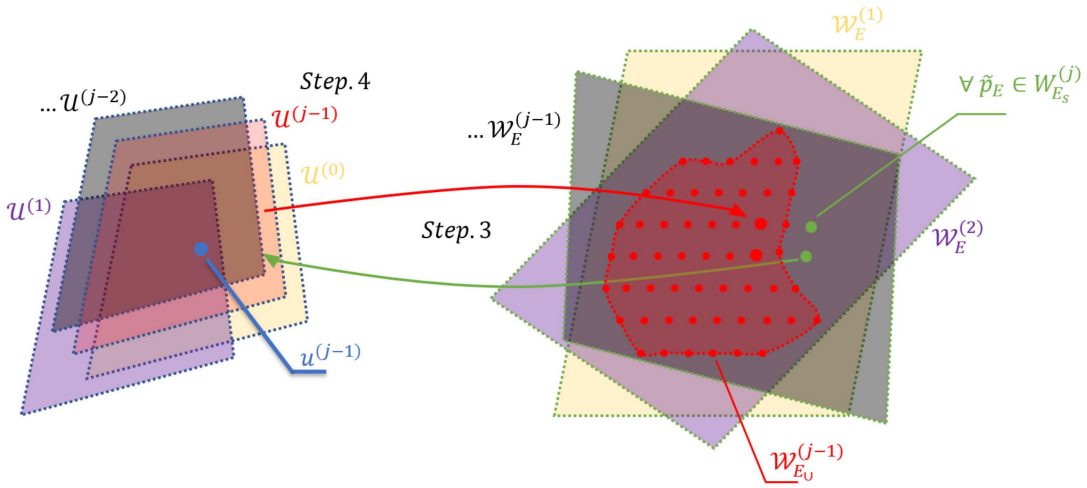


Figure 10: Iterative procedure and final result.

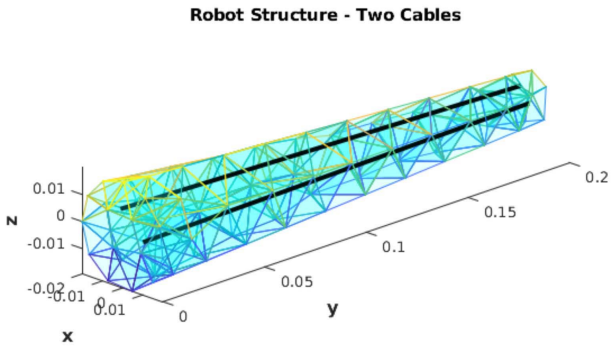


(a) Soft Robot Structure - Two Cables.

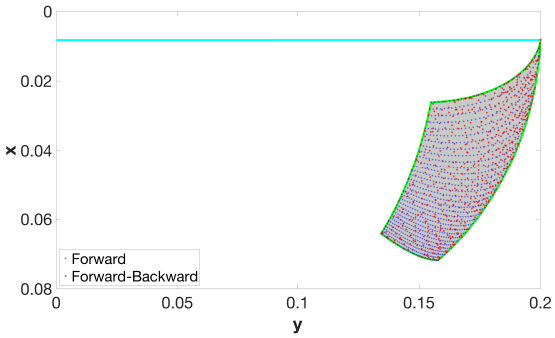


(b) $Oxy$ plane view of $\mathcal{W}_E$.

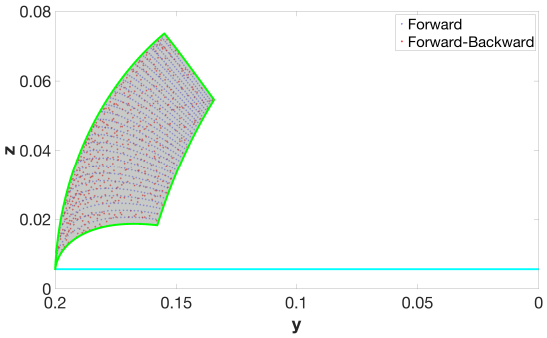


(c) $Ozy$ plane view of $\mathcal{W}_E$.

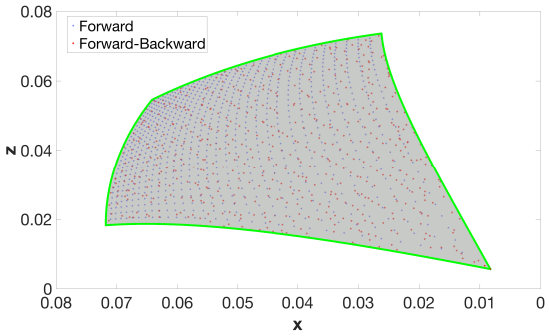


(d) $Ozx$ plane view of $\mathcal{W}_E$.

Figure 11: Scenario 1 - $\mathcal{W}_E$ estimation via forward approach (blue points) and forward-backward (gray area) approach.

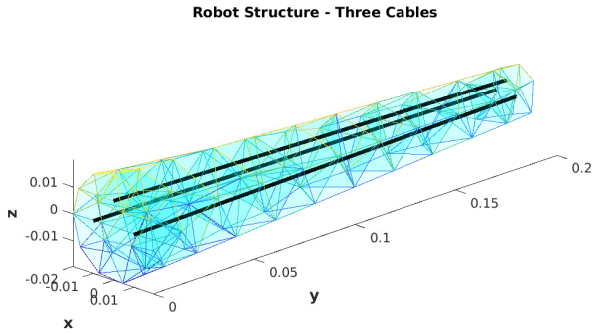


(a) Soft Robot Structure - Three Cables.

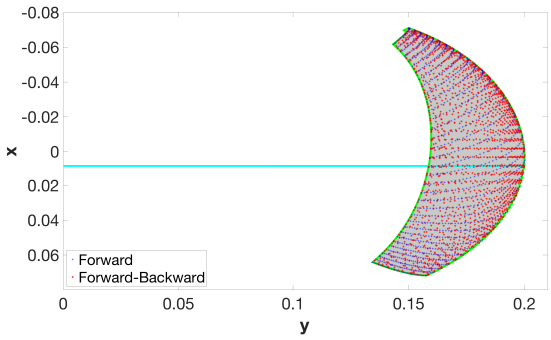


(b) $Oxy$ plane view of $\mathcal{W}_E$.

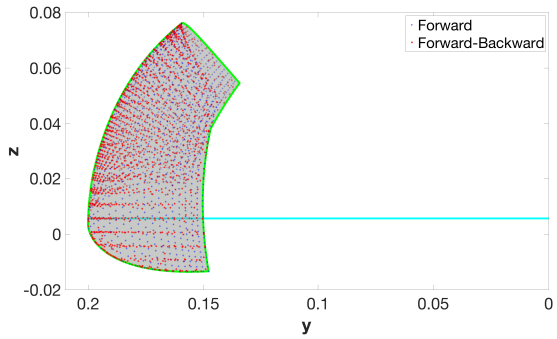


(c) $Ozy$ plane view of $\mathcal{W}_E$.

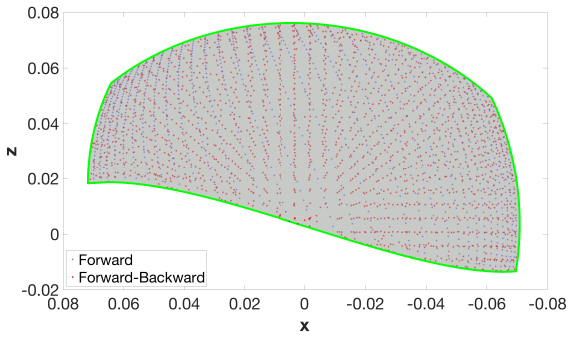


(d) $Ozx$ plane view of $\mathcal{W}_E$.

Figure 12: Scenario 2 - $\mathcal{W}_E$ estimation via forward approach (blue points) and forward-backward (gray area) approach.

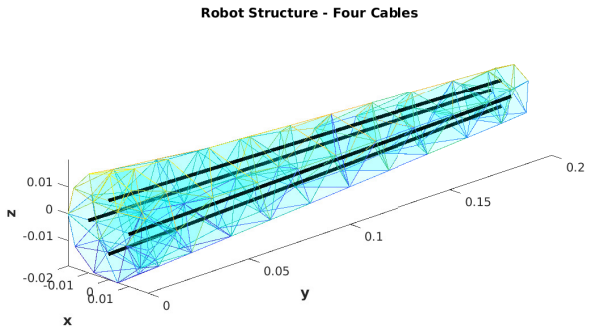


(a) Soft Robot Structure - Four Cables.

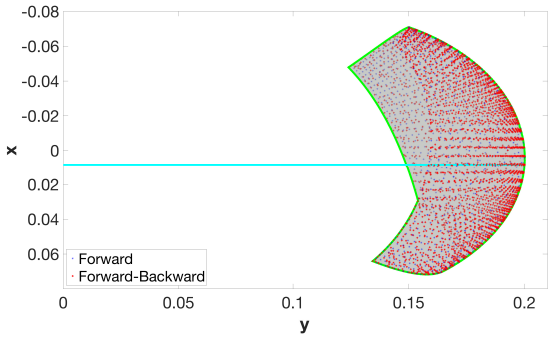


(b) $Oxy$ plane view of $\mathcal{W}_E$.

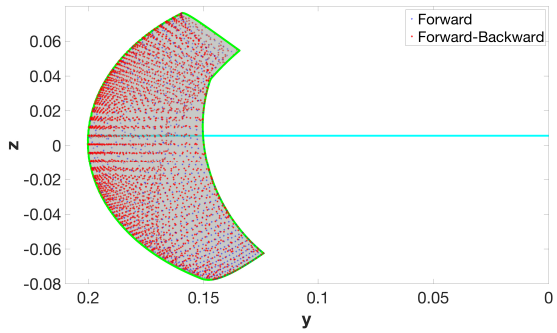


(c) $Ozy$ plane view of $\mathcal{W}_E$.

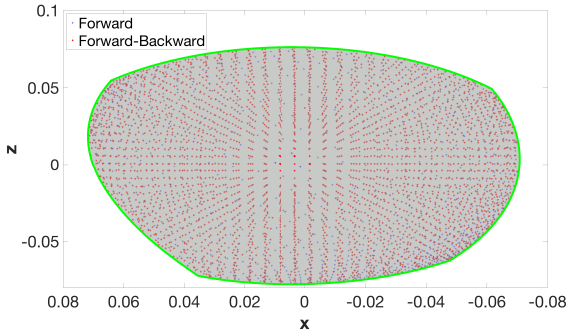


(d) $Ozx$ plane view of $\mathcal{W}_E$.

Figure 13: Scenario 3 - $\mathcal{W}_E$ estimation via forward approach (blue points) and forward-backward (gray area) approach.

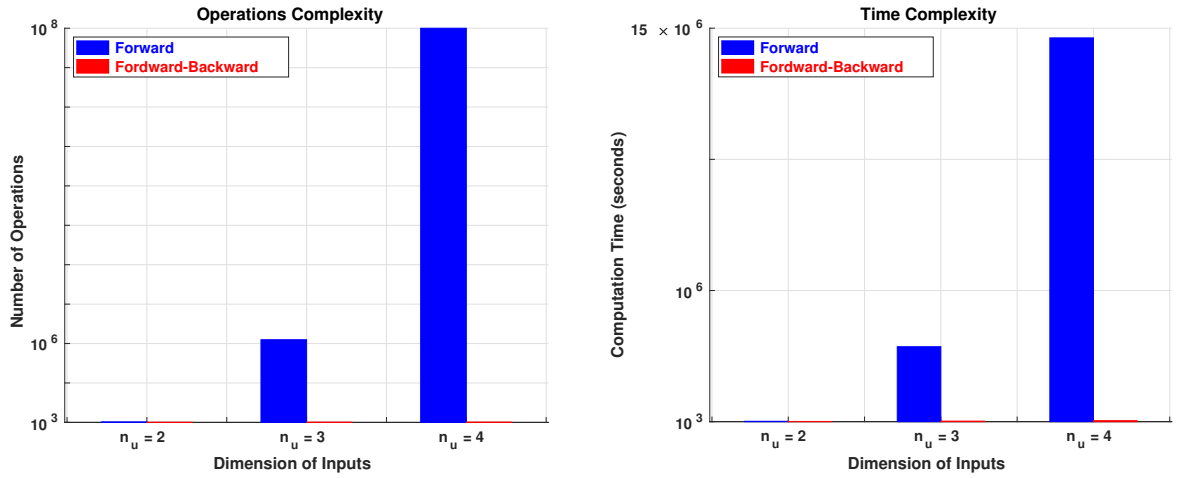


(a) Operations computation complexity.

(b) Time computation complexity

Figure 14: Operations and time computation complexity of the forward and forward-backward approach for the workspace estimation of soft robots.

Table 1: Operations and time computational complexity: forward vs forward-backward.

| | Operations | | Time (seconds) | |
|---|---|---|---|---|
| Scenario / Approach | Forward | Forward-Backward | Forward | Forward-Backward |
| First ($n_u = 2$) | $10^4$ | 635 | 1463 | 757 |
| Second ($n_u = 3$) | $10^6$ | 1941 | $\approx 1.46 \times 10^5$ | 2063 |
| Third ($n_u = 4$) | $10^8$ | 3667 | $\approx 1.46 \times 10^7$ | 3733 |

# References


[1] S. Cetinkunt and W. J. Book, "Performance limitations of joint variable-feedback controllers due to manipulator structural flexibility," *IEEE Transactions on Robotics and Automation*, vol. 6, no. 2, pp. 219–231, 1990.

[2] S. Yim and M. Sitti, "Design and rolling locomotion of a magnetically actuated soft capsule endoscope," *IEEE Transactions on Robotics*, vol. 28, no. 1, pp. 183–194, 2012.

[3] C. J. Payne, I. Wamala, C. Abah, T. Thalhofer, M. Saeed, D. Bautista-Salinas, M. A. Horvath, N. V. Vasilyev, E. T. Roche, F. A. Pigula *et al.*, "An implantable extracardiac soft robotic device for the failing heart: Mechanical coupling and synchronization," *Soft robotics*, vol. 4, no. 3, pp. 241–250, 2017.

[4] F. Iida and C. Laschi, "Soft robotics: challenges and perspectives," *Procedia Computer Science*, vol. 7, pp. 99–102, 2011.

[5] R. F. Shepherd, F. Ilievski, W. Choi, S. A. Morin, A. A. Stokes, A. D. Mazzeo, X. Chen, M. Wang, and G. M. Whitesides, "Multigait soft robot," *Proceedings of the national academy of sciences*, vol. 108, no. 51, pp. 20 400–20 403, 2011.

[6] D. Rus and M. T. Tolley, "Design, fabrication and control of soft robots," *Nature*, vol. 521, no. 7553, pp. 467–475, 2015.

[7] J. Snyman, L. Du Plessis, and J. Duffy, "An optimization approach to the determination of the boundaries of manipulator workspaces," *Journal of Mechanical Design*, vol. 122, no. 4, pp. 447–456, 2000.

[8] E. J. Haug, C.-M. Luh, F. A. Adkins, and J.-Y. Wang, "Numerical algorithms for mapping boundaries of manipulator workspaces," *Journal of Mechanical Design*, vol. 118, no. 2, pp. 228–234, 1996.

[9] K. Abdel-Malek and H.-J. Yeh, "Analytical boundary of the workspace for general3-dof mechanisms," *The International Journal of Robotics Research*, vol. 16, no. 2, pp. 198–213, 1997.

[10] M. Gouttefarde, D. Daney, and J.-P. Merlet, "Interval-analysis-based determination of the wrench-feasible workspace of parallel cable-driven robots," *IEEE Transactions on Robotics*, vol. 27, no. 1, pp. 1–13, 2010.

[11] J.-P. Merlet, "On the workspace of suspended cable-driven parallel robots," in *2016 IEEE International Conference on Robotics and Automation (ICRA)*. IEEE, 2016, pp. 841–846.

[12] A. Berti, J.-P. Merlet, and M. Carricato, "Workspace analysis of redundant cable-suspended parallel robots," in *Cable-Driven Parallel Robots*. Springer, 2015, pp. 41–53.

[13] R. J. Webster III and B. A. Jones, "Design and kinematic modeling of constant curvature continuum robots: A review," *The International Journal of Robotics Research*, vol. 29, no. 13, pp. 1661–1683, 2010.

[14] F. Renda, F. Boyer, J. Dias, and L. Seneviratne, "Discrete cosserat approach for multisection soft manipulator dynamics," *IEEE Transactions on Robotics*, vol. 34, no. 6, pp. 1518–1533, 2018.

[15] C. Duriez, "Control of elastic soft robots based on real-time finite element method," in *2013 IEEE international conference on robotics and automation*. IEEE, 2013, pp. 3982–3987.

[16] S. S. Rao, *The finite element method in engineering*. Butterworth-heinemann, 2017.

[17] L. Jaulin, M. Kieffer, O. Didrit, and E. Walter, "Interval analysis," in *Applied Interval Analysis*. Springer, 2001, pp. 11–43.

[18] W. Amehri, G. Zheng, and A. Kruszewski, "Fem based workspace estimation for soft robots: A forward-backward interval analysis approach," in *2020 3rd IEEE International Conference on Soft Robotics (RoboSoft)*. IEEE, 2020, pp. 170–175.

[19] T. M. Bieze, F. Largilliere, A. Kruszewski, Z. Zhang, R. Merzouki, and C. Duriez, "Finite element method-based kinematics and closed-loop control of soft, continuum manipulators," *Soft robotics*, vol. 5, no. 3, pp. 348–364, 2018.

[20] A. Rodríguez, E. Coevoet, and C. Duriez, "Real-time simulation of hydraulic components for interactive control of soft robots," in *2017 IEEE International Conference on Robotics and Automation (ICRA)*. IEEE, 2017, pp. 4953–4958.

[21] J. Reddy, *An introduction to the finite element method*. McGraw-Hill New York, USA, 2013, vol. 1221.

[22] Z. Zhang, T. M. Bieze, J. Dequidt, A. Kruszewski, and C. Duriez, "Visual servoing control of soft robots based on finite element model," in *2017 IEEE/RSJ International Conference on Intelligent Robots and Systems (IROS)*. IEEE, 2017, pp. 2895–2901.

[23] G. Zheng, O. Goury, M. Thieffry, A. Kruszewski, and C. Duriez, "Controllability pre-verification of silicone soft robots based on finite-element method," in *2019 International Conference on Robotics and Automation (ICRA)*. IEEE, 2019, pp. 7395–7400.

[24] G. Zheng, D. Efimov, and W. Perruquetti, "Design of interval observer for a class of uncertain unobservable nonlinear systems," *Automatica*, vol. 63, pp. 167–174, 2016.